[CANCER RESEARCH 62, 4909–4915, September 1, 2002]

dUTPase and Uracil-DNA Glycosylase Are Central Modulators of Antifolate Toxicity in *Saccharomyces cerevisiae*[1]

Beverly A. Tinkelenberg, Michael J. Hansbury, and Robert D. Ladner[2]

Department of Molecular Biology, University of Medicine and Dentistry of New Jersey, School of Osteopathic Medicine, Stratford, New Jersey 08084 [B. A. T., R. D. L.], and Oncology Research, GlaxoSmithKline, King of Prussia, Pennsylvania 19406 [M. J. H.]

ABSTRACT

The thymidylate synthase reaction remains an important target for widely used anticancer agents; however, the clinical utility of these drugs is limited by the occurrence of cellular resistance. Despite the considerable amount of information available regarding mechanisms of drug action, the relative significance of downstream events that result in lethality remains unclear. In this study, we have developed a model system using the budding yeast *Saccharomyces cerevisiae* to dissect the influence of dUMP misincorporation into DNA as a contributing mechanism of cytotoxicity induced by antifolate agents. The activities of dUTPase and uracil-DNA glycosylase, key enzymes in uracil-DNA metabolism, were diminished or augmented, and the manipulated strains were analyzed for biochemical endpoints of toxicity. Cells overexpressing dUTPase were protected from cytotoxicity by their ability to prevent dUTP pool expansion and were able to recover from an early S-phase checkpoint arrest. In contrast, depletion of dUTPase activity leads to the accumulation of dUTP pools and enhanced sensitivity to antifolates. These cells were also arrested in early S-phase and were unable to complete DNA replication after drug withdrawal, resulting in lethality. Inactivation of uracil base excision repair induced partial resistance to early cytotoxicity (within 10 h); however, lethality ultimately resulted at later time points (12–24 h), presumably because of the detrimental effects of stable uracil misincorporation. Although these cells were able to complete replication with uracil-substituted DNA, they arrested at the G_2-M phase. This finding may represent a novel mechanism by which the G_2-M checkpoint is signaled by the presence of uracil-substituted DNA. Together these data provide both genetic and biochemical evidence demonstrating that lethality from antifolates in yeast is primarily dependent on uracil misincorporation into DNA, and that uracil-independent mechanisms associated with dTTP depletion play a minor role. Our findings indicate that the relative expression levels of both dUTPase and uracil-DNA glycosylase can have great influence over the efficacy of thymidylate synthase-directed chemotherapy, thereby enhancing the candidacy of these proteins as prognostic markers and alternative targets for therapeutic development.

INTRODUCTION

Thymidylate metabolism is an important target of widely used anticancer agents that are used to combat a variety of neoplastic diseases including head and neck, breast, and gastrointestinal cancers (1). Chemotherapeutic agents that target this pathway act by inhibiting the TS[3] reaction that catalyzes the reductive methylation of dUMP to dTMP. Inhibitors of this reaction include the fluoropyrimidine class of anticancer agents (FdUMP being the active metabolite) and TS-specific quinazoline antifolates [*i.e.*, ZD1694 (Tomudex) and ZD9331] that directly inhibit the TS enzyme. Antifolate inhibitors of dihydrofolate reductase, such as aminopterin and methotrexate, can indirectly block dTMP production by depleting tetrahydrofolate pools required for the TS reaction. Inhibition of TS leads to a series of complex biochemical events that ultimately result in DNA damage and cytotoxicity, often referred to as thymineless death (2).

Analysis of the downstream biochemical consequences of TS inhibition demonstrates that depletion of dTTP pools triggers feedback mechanisms that induce the accumulation of dUMP and imbalance in deoxynucleotide triphosphate pools (3). Although the exact biochemical basis for toxicity in TS-inhibited cells remains unclear, it is likely to result from the profound effects of nucleotide precursor imbalance (3). Several mechanisms involving imbalance in particular nucleotides have been proposed including dTTP pool deprivation (4), elevation in dATP pools (5, 6), lowered dGTP pools (7), and dUTP pool accumulation, resulting in aberrant uracil misincorporation into DNA (8). Although many researchers have accepted uracil misincorporation as one component of TS inhibitor-based lethality, the relative significance of this pathway in mediating cell death has not been fully established.

During TS inhibition, dTTP pools are depleted, and dUMP pools accumulate behind the metabolic blockade. dUMP is subsequently phosphorylated by the action of mono- and dinucleotide kinases to form dUTP. If the build-up of dUTP overwhelms cellular dUTPase activity, the enzyme responsible for eliminating dUTP from the cell, dUTP pools will accumulate and can be used in place of dTTP by DNA polymerase during replication and repair (9). Under these conditions, the cell experiences detrimental cycles of uracil misincorporation and uracil-DNA glycosylase-mediated repair, resulting in catastrophic DNA damage and cell death (8, 10–12).

Studies aimed at determining the significance of uracil misincorporation have shown that exogenously expressed *Escherichia coli* dUTPase partially protects HT29 colon cancer cells from 5-fluorodeoxyuridine-induced DNA damage and toxicity (13). However, dUTPase overexpression did not protect HuTu80 cells from 5-fluorodeoxyuridine treatment, suggesting that this is not a consistent finding. Additionally, investigation in other cell culture models demonstrates that dUTP pools do not accumulate in all cell lines that are sensitive to TS inhibition (8). These data suggest that uracil misincorporation may not be the critical event resulting in lethality, and that other mechanisms, such as dTTP pool depletion itself, may play a more dominant role (8, 14). Thus, despite considerable effort to elucidate the underlying mechanisms responsible for toxicity in TS inhibited cells, the precise mechanisms remain controversial.

The budding yeast *Saccharomyces cerevisiae* offers a powerful model to examine the action of anticancer agents and clarify the contribution of a specific gene or metabolic pathway in regulating sensitivity or resistance. Studies performed in budding yeast have suggested the role of uracil misincorporation as the mechanistic basis of antifolate toxicity; however, direct biochemical evidence demonstrating its involvement has not been shown (15). The purpose of this study was to use yeast as a model to determine the significance of aberrant uracil-DNA metabolism as a mechanism of cytotoxicity after TS inhibition by antifolate agents. To address this issue, we sought to

Received 2/27/02; accepted 6/25/02.

The costs of publication of this article were defrayed in part by the payment of page charges. This article must therefore be hereby marked *advertisement* in accordance with 18 U.S.C. Section 1734 solely to indicate this fact.

[1] This research was supported by the NIH Grant CA83861 from the National Cancer Institute and by the Foundation of UMDNJ Grant 17-01 (to R. D. L.).

[2] To whom requests for reprints should be addressed, at Department of Molecular Biology, UMDNJ-SOM, 2 Medical Center Drive, Stratford, NJ 08084. Phone: (856) 566-6043; Fax: (856) 566-6291; E-mail: ladner@umdnj.edu.

[3] The abbreviations used are: TS, thymidylate synthase; 5-FOA, 5-fluoro-orotic acid; A + S, 100 μg/ml aminopterin and 5 mg/ml sulfanilamide; PFGE, pulsed field gel electrophoresis; ORF, open reading frame; FACS, fluorescence-activated cell sorting; Ts, temperature sensitive.

diminish and augment the cellular activities of dUTPase and uracil-DNA glycosylase to understand their influence on antifolate-mediated lethality. The TS reaction represents the sole source of dTMP in these organisms, allowing for the unambiguous analysis of the consequences of TS inhibition. Through a series of genetic and biochemical-based analyses, we demonstrate that aberrant uracil misincorporation and excision plays a dominant role in antifolate toxicity, and that dTTP pool depletion alone does not mediate extreme lethality in yeast. Our data suggest that the relative cellular expression of dUTPase and uracil-DNA glycosylase can have profound effects on the ability of cells to respond to antifolates.

MATERIALS AND METHODS

Yeast Growth Conditions. Yeast cells were grown at 30°C. SC medium was formulated according to Burke *et al.* (16). Carbon sources (glucose, raffinose, and galactose; 2%) are indicated in the individual experiments. Raffinose was used as a noninducing/nonrepressing carbon source of the *GAL-1* promoter. Galactose was used to induce expression from the *GAL1* promoter. Where indicated, 5-FOA was used at 0.1%, and nocodazole was used at 10 μg/ml.

Antifolate Killing Assays. For antifolate killing, cells were grown to log phase in SC −Ura −Leu GAL (containing galactose), whereupon the cell density was adjusted to 5×10^6 cells/ml, and the medium was replaced with SC −Ura −Leu GAL + A + S, unless otherwise indicated. Aliquots were withdrawn and washed, and a determined number of cells was plated onto SC −Ura −Leu GAL agar at timed intervals and allowed to grow for several days at 30°C. Statistical analysis of results was performed by one-way ANOVA using GraphPad Prism software.

Synchronization of Cells in G_1. Strains were grown to log phase in SC −Ura −Leu GAL and treated with 1.5 μM α-factor (Sigma) for 4 h. Cells were then harvested, washed, and resuspended in SC −Ura −Leu GAL + A + S as indicated in the individual experiments.

Nucleotide Pool Assays. Deoxynucleotide triphosphate pool sizes were determined by an enzymatic method first described by Sherman and Fyfe (17). dTTP and dUTP pools were determined independently by preincubating cellular extracts with or without recombinant dUTPase (18). Yeast cells (5×10^6) were harvested at timed intervals, washed, resuspended in 100 μl of 10% trichloroacetic acid, and processed as described.

PFGE-based Determination of Replication Intermediates and Detection of Uracil in DNA. At timed intervals, 1.2×10^8 cells were harvested by centrifugation, washed, resuspended in 500 μl of 10 mM Tris (pH 7.2), 20 mM NaCl, 50 mM EDTA plus 6 μl of Zymolyase (10 mg/ml), and incubated for 60 s at 37°C. The cell suspension was then mixed with 500 μl of 2% pulsed field certified agarose (Bio-Rad) premelted and equilibrated to 50°C, and transferred into plug molds. After solidification, the plugs were incubated in 0.5 M EDTA, 10 mM Tris (pH 7.5) for 8 h at 37°C. After incubation, plugs were processed for PFGE as per the manufacturer's recommendations (Bio-Rad). Separation of chromosomal DNA was carried out over 11 h at 120 V with a switch time of 1–6 s, and chromosomes were visualized with ethidium bromide. To detect uracil in DNA, plugs were first incubated in 1 mM phenylmethylsulfonyl fluoride for 1 h at room temp and then equilibrated in Ung1 digestion buffer [50 mM Tris (pH 7.6) and 0.2 M NaCl]. Plugs were digested overnight with recombinant uracil-DNA glycosylase (Ung1; 200 ng/ml) and AP endonuclease (Apn1; 200 ng/ml) in 300 μl of Ung1 digestion buffer and then separated according to parameters described above. Recombinant Ung1 expression and purification have been described previously (19). The ORF of the major class II AP endonuclease from yeast (*APN1*) was PCR amplified from total genomic DNA, and the resulting fragment was cloned into the expression vector pProEx Htb (Life Technologies, Inc.). Recombinant Apn1 protein was overexpressed in DH5α cells and affinity purified by use of a Ni-NTA Agarose (Qiagen) as per the manufacturer's recommendations.

FACS Analysis. At timed intervals, 5×10^6 cells were harvested and resuspended in 250 μl of 0.25 M Tris (pH 7.5). Cells were then processed for FACS as described (20). Samples were analyzed for fluorescence content on a FACScan flow cytometer (Becton Dickinson).

Strain and Plasmid Construction. Refer to Table 1 for details on all plasmids and yeast strains generated in this study. To construct a yeast strain suitable for generating Ts mutants of the *DUT1* gene by PCR mutagenesis and plasmid shuffling, a Δ*dut1::HIS3/DUT1* diploid (BMY100) was made from MHY340 by standard gene disruption procedures (21). To suppress lethality from dUTPase deficiency, BMY100 was transformed with the *URA3* CEN plasmid, pBAM10, which contains the human dUTPase ORF (*hDUT-N*) under the control of the *DUT1*promoter (see below). The resulting strain was sporulated, tetrads were dissected, and haploids harboring the pBAM10 plasmid were selected on SC −Ura medium. Strains containing the *DUT1* knockout were identified by the inability to grow on replica plates of SC −Ura supplemented with 5-FOA. To construct BMY102, BMY101 was transformed with pBAM11 (*CEN6 LEU2*-hDUT-N), and cells were plated on SC −Leu + 5-FOA to ensure the loss of the pBAM10 plasmid.

Table 1 *Strains and plasmids used in this study*

Strain	Genotype	Source
MHY340	*MATa/α ura3-52/ura3-52 leu2Δ1/leu2Δ1 his3Δ200/ his3Δ200 ade2/ADE2 ade3/ADE3 lys2LYS2 trp1/ TRP1*	M. Henry (UMDNJ)
BMY66	*MATa ura3-52 leu2Δ1 his3Δ200 trp1*	This study
BMY100	as MHY340 Δ*dut1*::*HIS3/DUT1*	This study
BMY101	as BMY66 Δ*dut1*::*HIS3* + pBAM10	This study
BMY102	as BMY66 Δ*dut1*::*HIS3* + pBAM11	This study
BMY106	as BMY66 Δ*dut1*::*HIS3* + pBAM11 + pPS293	This study
BMY107	as BMY66 Δ*dut1*::*HIS3* + pBAM11 + pBAM12	This study
BMY108	as BMY66 Δ*dut1*::*HIS3* + pBAM11 + pBAM13	This study
BMY109	as BMY66 Δ*dut1*::*HIS3* + pBAM11 + pBAM14	This study
BMY114	as BMY102 Δ*ung1*::*TRP1* + pPS293	This study
BMY119	as BMY102 Δ*ung1*::*TRP1* + pBAM12	This study
Plasmid	**Relevant markers**	**Source**
pRS315	Amp^r *CEN6 LEU2*	M. Henry
pRS316	Amp^r *CEN6 URA3*	M. Henry
pPS293	Amp^r *2μ URA3 GAL1* promoter	M. Henry
pBAM10	Amp^r *CEN6 URA3—hDUT-N*	This study
pBAM11	Amp^r *CEN6 LEU2—hDUT-N*	This study
pBAM12	Amp^r *2μ URA3 GAL1—DUT1*	This study
pBAM13	Amp^r *2μ URA3 GAL1—UNG1*	This study
pBAM14	Amp^r *2μ URA3 GAL1—Ugi*	This study

The *hDUT-N-DUT1* promoter expression cassettes were generated by flanking the *hDUT-N* ORF between *DUT-1* gene sequences 0.9 kb upstream and 0.7 kb downstream of the coding region. The human *DUT-N* ORF was PCR amplified from the gene cloned previously (22), and *DUT-1* flanking sequences were PCR amplified from yeast genomic DNA. Each PCR fragment was sequentially cloned into pBluescript (pBS-), and the entire *hDUT-N-DUT1* promoter expression cassette was subcloned using *Sst*I and *Xba*I sites into either pRS316 (*URA3*) or pRS315 (*LEU2*) generating pBAM10 and pBAM11, respectively.

The ORFs of the yeast genes encoding dUTPase (*DUT1*) and uracil-DNA glycosylase (*UNG1*) were PCR amplified from total genomic DNA. The ORF of the *Bacillus subtilis* bacteriophage PBS2-encoded uracil-DNA glycosylase inhibitor protein (*Ugi*) was PCR amplified from the gene cloned previously (19). The resulting PCR products were cloned into pGEM-3Z (Promega) and sequenced to verify lack of mutation. The individual ORFs were then subcloned into the galactose-inducible expression vector pPS293 (2μ *URA3 GAL1* promoter), generating pBAM12–14 (see Table 1). Each plasmid construct and empty pPS293 was then transformed into BMY102 and selected on SC −Leu −Ura, generating BMY106–109. Knockout of the *UNG1* gene was performed in BMY106 using the *TRP1* gene as a selectable marker (21), generating BMY114 (Δ*ung1*). Gene disruption of *UNG1* and *Ung1* inhibition by Ugi expression was confirmed by Southern blot and an *in vitro* uracil-DNA cleavage assay (23). Overexpression of *DUT1* and *UNG1* was measured by *in vitro* enzymatic assays as described (19, 22). Enzymatic activity in soluble whole-cell extracts was calculated as fold increase over endogenous levels of dUTPase and uracil-DNA glycosylase. Endogenous levels of Dut1 activity in BMY107 were determined to be 1.4 pmol of dUTP cleaved/min/μg of protein. Endogenous levels of Ung1 activity in BMY108 were determined to be 0.4 pmol of uracil cleaved/min/μg of protein.

RESULTS

A Yeast Model for Uracil-DNA Metabolism. To investigate the significance of aberrant uracil misincorporation as a mechanism of

thymineless death, we set out to determine the influence of dUTP metabolism and uracil-DNA repair on antifolate treatment in *S. cerevisiae*. Our goal was to generate a series of strains possessing depleted or elevated levels of dUTPase and uracil-DNA glycosylase and to analyze their effect on the biochemical events after treatment with A + S.

Because dUTPase is an essential gene, it is not possible to analyze the effects of a dUTPase-deficient strain. Therefore, we sought to generate Ts mutants of *DUT-1* to assess the influence of a compromised dUTPase function on toxicity. To generate Ts alleles of *DUT-1*, we attempted PCR-based mutagenesis and plasmid shuffling. To perform this experiment, we constructed a *dut1*null strain, BMY101, which was kept alive by the human dUTPase gene, *hDUT-N*, on a *URA3 CEN* plasmid, pBAM10. Although we were unable to generate Ts alleles of *DUT1* by this approach, we noticed that BMY101 was greatly sensitized to A + S treatment (3% survival after 8 h) compared with an isogenic control strain, BMY66, that is wild type at the *DUT1* locus (60% survival after 8 h; data not shown). Analysis of dUTPase in these strains by enzymatic assay revealed that BMY101 contains 5-fold less dUTPase activity compared with BMY66, suggesting that the relative level of dUTPase activity can greatly influence antifolate cytotoxicity. We also noted that BMY101 accumulated dUTP pools subsequent to A + S treatment, whereas BMY66 did not, further implicating uracil-DNA metabolism as a key player in mediating toxicity.

To overexpress dUTPase and uracil-DNA glycosylase, the ORFs of the yeast *DUT1* and *UNG1* genes were cloned into a *URA3* 2μ plasmid under the control of the *GAL1* promoter (pPS293), generating pBAM12 and pBAM13, respectively. These plasmids, including empty vector, were then transformed into BMY102 cells (isogenic with BMY101 with *hDUT-N* on a *LEU2 CEN* plasmid, pBAM11), generating BMY106 (p*GAL-empty*), BMY107 (p*GAL-DUT1*), and BMY108 (p*GAL-UNG1*). Expression of dUTPase and uracil-DNA glycosylase was induced by growing cells in galactose (SC −Ura −Leu GAL), and enzyme activity was monitored in total cell extracts as described previously (19, 22). Expression of Dut1 increased 50-fold over the endogenous cellular activity 8 h after galactose induction, whereas Ung1 activity increased 15-fold.

To eliminate uracil-DNA glycosylase activity, two independent approaches were used:

(*a*) We inhibited the cellular Ung1 activity by overexpressing the PBS2 bacteriophage-encoded uracil-DNA glycosylase inhibitor protein, Ugi. This approach has been used successfully to inhibit uracil-DNA glycosylase activity in human cells (24). The Ugi ORF was cloned into pPS293, resulting in pBAM14, which was subsequently transformed into BMY102, generating BMY109 (p*GAL-Ugi*).

(*b*) We constructed an *ung1* null strain in the BMY106 background, generating BMY114 (Δ*ung1*). The deletion of uracil-DNA glycosylase in the Δ*ung1* strain and the inhibition of Ung1 activity by expression of Ugi were confirmed by Southern blot and enzymatic assay (data not shown).

To ensure that the strains described above had similar growth characteristics, cells were grown to log phase in SC −Leu −Ura GAL medium and monitored microscopically during various time periods. All strains exhibited identical doubling times over an 8-h time course (data not shown). Therefore, analysis of antifolate response is not confounded by strain-specific differences in growth properties.

The Enzymes of Uracil-DNA Metabolism Influence Lethality Induced by Antifolates. To examine the influence of dUTPase and uracil-DNA glycosylase activities on sensitivity to antifolate treatment, we determined the relative survival curves of the strains described above during various time periods of A + S treatment under galactose-induced conditions. The survival curves for each strain are presented in Fig. 1. The untreated control strain containing empty vector, BMY106 (p*GAL-empty*), showed no loss of viability over 24 h, as did all of the untreated expression strains tested (data not shown). In contrast, A + S treatment induced severe lethality in this strain corresponding to <2% survival at 24 h. Overexpression of dUTPase led to a dramatic increase in resistance to antifolates throughout the time course. At 24 h of drug treatment, the survival of BMY107 (p*GAL-DUT1*) was 25-fold greater than its isogenic control strain, BMY106 (p*GAL-empty*). The difference in survival between these two strains provides strong evidence that cell death attributable to A + S is mediated primarily through a dUTP-dependent mechanism.

The strain overexpressing Ung1, BMY108 (p*GAL-UNG1*), exhibits a similar loss of viability as p*GAL-empty* throughout the 24-h time course. However, when *UNG1* is deleted, BMY114 (Δ*ung1*), or inactivated by Ugi, BMY109 (p*GAL-Ugi*) cells experience a significant protection from lethality 4–10 h after A + S addition when compared with the drug-treated isogenic control strain, p*GAL-empty* ($P < 0.004$ for each time point). Survival in these strains deteriorates after 12 h of A + S treatment, where it becomes nearly indistinguishable from p*GAL-empty*. These data suggest that the uracil-DNA repair system plays an important role in mediating cell killing, particularly at early time points. Lethality at later time points in the *ung*- background

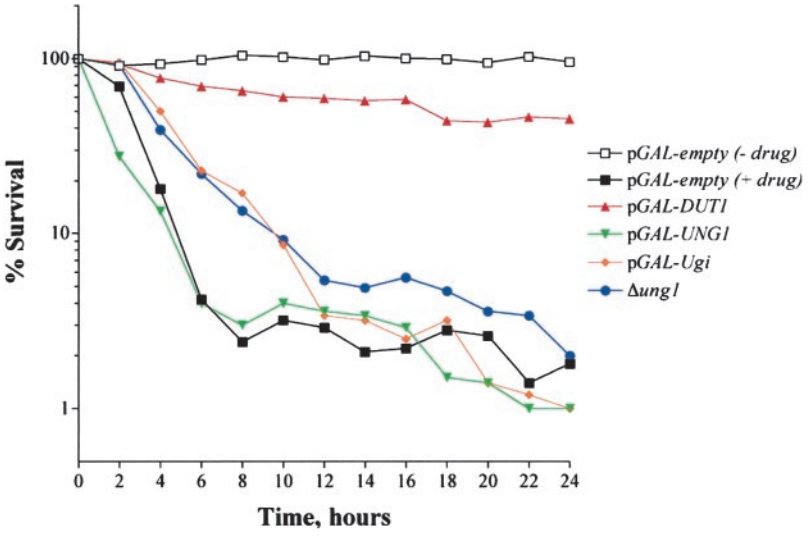

Fig. 1. Effects of antifolates on viability. Asynchronous cultures in mid-log phase were treated with 100 μg/ml aminopterin plus 5 mg/ml sulfanilamide. At 2-h intervals, aliquots were withdrawn, and the cells were washed and plated on SC −Ura −Leu agar medium to determine viability. Colonies were scored after 2–3 days of incubation at 30°C. □, untreated BMY106 (Δ*dut1::HIS3* + pBAM11 + pPS293); ■, treated BMY106 (Δ*dut1::HIS3* + pBAM11 + pPS293); ▲, BMY107 (Δ*dut1::HIS3* + pBAM11 + p*GAL-DUT1*); ▼, BMY108 (Δ*dut1::HIS3* + pBAM11 + p*GAL-UNG1*); ♦, BMY109 (Δ*dut1::HIS3* + pBAM11 + p*GAL-Ugi*); ●, BMY114 (Δ*dut1::HIS3* Δ*ung1::TRP1* + pPS293).

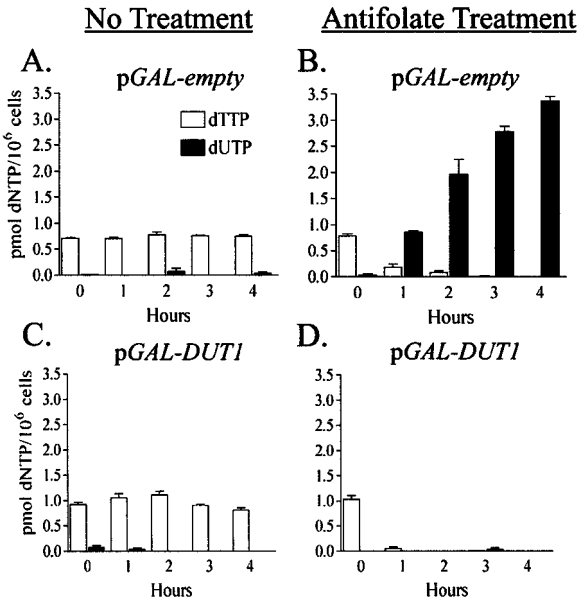

Fig. 2. TTP and dUTP pool analysis of antifolate-treated cells. Nucleotide pools were determined in yeast cells that were either untreated or treated with 100 μg/ml aminopterin plus 5 mg/ml sulfanilamide over a 4-h time course. At timed intervals, cells were harvested and washed, and dUTP and dTTP pools were determined by a DNA polymerase-based assay (see "Materials and Methods"). *Bars*, SD. *A*, untreated control, BMY106 (Δ*dut1::HIS3* + pBAM11 + pPS293). *B*, treated control, BMY106. *C*, untreated BMY107 (Δ*dut1::HIS3* + pBAM11 + p*GAL-DUT1*); *D*, treated BMY107. (Results from BMY108, BMY109, and BMY114 resemble those from the control strain, BMY106, and are not shown.)

may be attributed to the detrimental effects of stable uracil misincorporation into DNA. Overexpression of *UNG1* does not result in greater lethality, suggesting that this enzyme is already expressed at saturating concentrations in terms of mediating DNA damage. To determine the mechanistic basis for the observed viability profiles, we performed subsequent biochemical analysis of the metabolic endpoints of the uracil-DNA pathway.

Elevated Expression of dUTPase Abrogates dUTP Pool Expansion in the Presence of Antifolates. The model of uracil-mediated cytotoxicity suggests that when dTMP synthesis is inhibited by antifolates, dTTP pools are depleted, dUMP pools accumulate, and dUMP is converted to dUTP by mono- and diphosphate kinases. If dUTPase is overwhelmed, dUTP pools may accumulate and be used by DNA polymerases in place of dTTP. To evaluate the significance of dUTP pool accumulation on antifolate toxicity, we measured dTTP and dUTP pool levels in our yeast strains.

Nucleotide pools were determined from yeast extracts over a 4-h time course. Results from experiments performed on BMY106 (p*GAL-empty*) and BMY107 (p*GAL-DUT1*) are presented in Fig. 2. Untreated cells from both strains contained dTTP levels ranging from 0.7 to 1.2 pmol/1 $\times$ 10^6 cells, whereas dUTP was virtually undetectable by this assay (Fig. 2, *A* and *C*). Cells treated with antifolates demonstrate a rapid decline in dTTP levels in both strains within 1 h, falling to $<$0.1 pmol/1 $\times$ 10^6 cells (Fig. 2, *B* and *D*). In p*GAL-empty*, dUTP levels accumulate to 3.3 $\pm$ 0.12 pmol/1 $\times$ 10^6 cells within 4 h (Fig. 2*B*). This represents $>$33:1 increase in the dUTP:dTTP ratio after 4 h of antifolate treatment. In contrast, when dUTPase was overexpressed in this system (p*GAL-DUT1*), both dTTP and dUTP were undetectable in our assay ($<$0.1 pmol/1 $\times$ 10^6 cells) within 3 h (Fig. 2*D*). These data demonstrate that dUTPase overexpression effectively suppresses dUTP pool expansion and confirm that severe antifolate toxicity correlates with dUTP status in the cell. Nucleotide pools determined for BMY108, BMY109, and BMY114 were essentially identical to the results obtained from the control strain, BMY106 (data not shown).

dUTPase and Uracil-DNA Glycosylase Activities Influence Checkpoint Response to Antifolates. To investigate cell cycle responses to the modulation of nucleotide pools and uracil-DNA repair status in antifolate-treated cells, we monitored progression through the cell cycle using FACS. Analysis was performed over a 6-h time course of antifolate treatment, and results of these experiments are presented in Fig. 3. Subsequent to drug treatment, the p*GAL-empty*, p*GAL-DUT1*, and p*GAL-UNG1* strains exhibit an early S-phase arrest, as indicated by a near 1C content of DNA. This early S-phase checkpoint in p*GAL-empty* and p*GAL-UNG1* is likely induced by DNA strand breaks, resulting from iterative cycles of uracil-base excision repair. Consistent with this hypothesis, yeast cells undergoing thymineless death demonstrate a decrease in the molecular weight of nuclear DNA, indicating the accumulation of DNA strand breaks (25). The early S-phase checkpoint initiated in the p*GAL-DUT1* strain may be attributed to stalled replication complexes caused by a lack of thymidine equivalent (dTTP or dUTP) available for DNA replication (see Fig. 2*D*). In contrast, the p*GAL-Ugi* and Δ*ung1* strains treated with antifolates both progress through S-phase and arrest in G_2-M as indicated by a 2C content of DNA. These data suggest that inactivation of Ung1 activity eliminates the antifolate-induced DNA damage that signals the early S-phase checkpoint, allowing cells to stably incorporate uracil into their DNA and complete replication. The unexpected G_2-M arrest observed in these cells may represent a novel signaling mechanism whereby the checkpoint is initiated by the occurrence of stably substituted uracil in DNA.

When dUTPase is overexpressed in the Δ*ung1* background (Δ*ung1*/p*GAL-DUT1*), cells arrest in early S-phase, identical to the *pGAL-DUT1* strain that contains wild-type levels of Ung1 (Fig. 3*F*). This result demonstrates that the early S-phase arrest is not attributable to low-level dUTP incorporation and Ung1-mediated misrepair and likely results from the combined effects of dTTP and dUTP pool depletion. Also of note is the observation that all of these strains

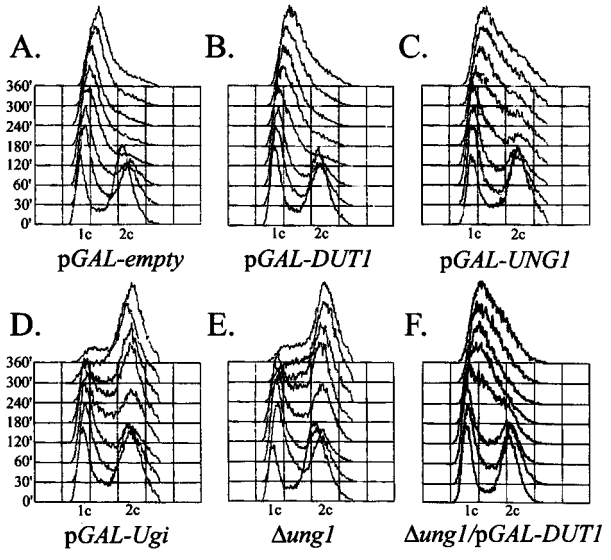

Fig. 3. Distinct cell cycle checkpoints are initiated by aberrant uracil-DNA metabolism. To determine cell cycle status upon antifolate treatment, yeast strains were analyzed for DNA content by FACS. Cells in the logarithmic phase were treated with A + S, harvested at various time points, and processed for FACS analysis. *A*, BMY106 (Δ*dut1::HIS3* + pBAM11 + pPS293). *B*, BMY107 (Δ*dut1::HIS3* + pBAM11 + p*GAL-DUT1*). *C*, BMY108 (Δ*dut1::HIS3* + pBAM11 + p*GAL-UNG1*). *D*, BMY109 (Δ*dut1::HIS3* + pBAM11 + p*GAL-Ugi*). *E*, BMY114 (Δ*dut1::HIS3* Δ*ung1::TRP1* + pPS293). *F*, BMY119 (Δ*dut1::HIS3* Δ*ung1::TRP1* + *p*GAL-DUT1).

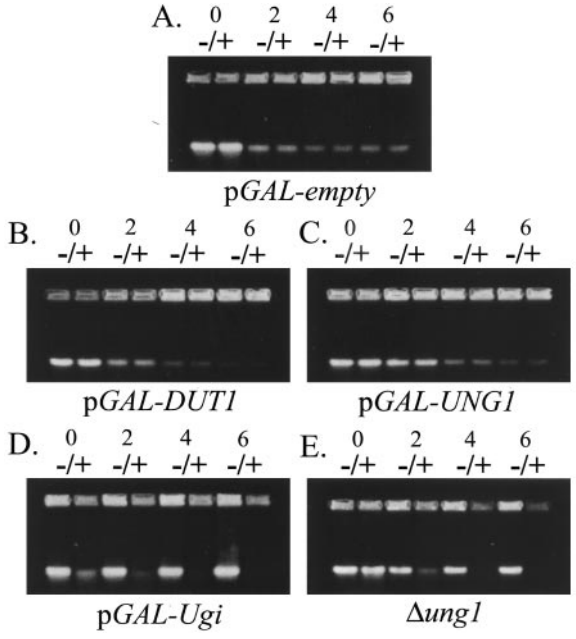

Fig. 4. Detection of replication intermediates and uracil misincorporation into DNA by PFGE. Cells in mid-log phase were treated with A + S, and 1.2×10^8 cells/ml plug were withdrawn at 0, 2, 4, and 6 h. Samples were processed for PFGE, and plugs were left untreated or subsequently digested with excess recombinant uracil-DNA glycosylase (Ung1) and apurinic/apyrimidinic endonuclease (Apn1). Treatment with Ung1/Apn1 results in the specific cleavage of DNA at uracil residues. DNA containing significant amounts of uracil is degraded, as indicated by a loss of chromosomal DNA on the gel. −/+, DNA-agarose plugs were either untreated or treated with Ung1 and Apn1. The pulsed field switch times during the electrophoresis process were altered so that all of the yeast chromosomes run together and appear as a single band on ethidium bromide stained agarose gels. *A*, BMY106 (Δ*dut1::HIS3* + pBAM11 + pPS293). *B*, BMY107 (Δ*dut1::HIS3* + pBAM11 + p*GAL-DUT1*). *C*, BMY108 (Δ*dut1::HIS3* + pBAM11 + p*GAL-UNG1*). *D*, BMY109 (Δ*dut1::HIS3* + pBAM11 + p*GAL-Ugi*). *E*, BMY114 (Δ*dut1::HIS3* Δ*ung1::TRP1* + pPS293).

displayed a dumbbell-shaped terminal morphology after antifolate treatment.

Antifolate Treatment Induces Uracil Misincorporation and the Formation of Replication Intermediates. Because FACS analysis only measures bulk DNA content, we wanted to examine chromosome structure and uracil content in antifolate-treated strains. We used PFGE as an experimental approach to examine the accumulation of persistent replication intermediates that may result from antifolate treatment. Using PFGE, replication intermediates (stalled or abandoned replication forks) can be detected by the migration patterns of chromosomal DNA on an agarose gel. Incompletely replicated chromosomes containing persistent replication intermediates fail to enter a pulsed-field gel because of the presence of open forks and replication bubbles that impede migration (26). We have modified this technique to detect the presence of uracil in DNA, where DNA plugs are predigested with recombinant Ung1 and apurinic/apyrimidinic endonuclease (Apn1) and then run on pulsed field gels. Uracil-containing DNA is differentiated from normal DNA by its sensitivity to degradation upon digestion with these enzymes. Results of these experiments are show in Fig. 4.

Antifolate treatment results in a time-dependent decrease in migrating DNA in the p*GAL-empty*, p*GAL-DUT1*, and p*GAL-UNG1* strains, indicating the formation of abnormal chromosomal structures or replication intermediates. All of these strains exhibit no detectable uracil in their residual migrating DNA, as evidenced by a lack of DNA degradation upon Ung1/Apn1 treatment. It is important to note, however, that this analysis does not rule out the possibility that the nonmigrating DNA may contain some uracil residues that are not detectable by this assay. Together, these data suggest that both uracil misincorporation followed by Ung1-mediated repair and the lack of a thymidine equivalent for replication (dTTP and dUTP) attributable to dUTPase overexpression lead to the formation of replication intermediates. These two mechanisms of generating abnormal DNA structure both induce an early S-phase checkpoint arrest; however, they have profoundly different outcomes in terms of survival.

In contrast, the p*GAL-Ugi* and Δ*ung1* strains appear to retain DNA of normal structure, as evidenced by the migration pattern of chromosomal DNA into the gel throughout the time course (Fig. 4, *D* and *E*). Additionally, these strains undergo a time-dependent, stable misincorporation of uracil into their DNA as demonstrated by the degradation induced by Ung1/Apn1 treatment. These data establish that, in the absence of Ung1 activity, uracil replaces thymidine during DNA synthesis in antifolate-treated cells. Uracil substitution allows for the completion of DNA replication, as shown by FACS, generating DNA of normal structure.

dUTPase-induced Resistance to Antifolates Results from Increased Recovery from Replicational Stress. Recovery from antifolate-induced checkpoint arrest varied greatly between the yeast strains tested in this study, as evidenced by dramatically different survival curves (Fig. 1). To determine whether lethality resulting from antifolate treatment is related to the ability to recover from persistent replication intermediates, we analyzed chromosomal structure by PFGE after drug was withdrawn. For these experiments, cells were treated with α-factor to synchronize cells in G_1 for a more uniform response to drug. Cells were then released from α-factor into medium containing A + S for 2 h and transferred into fresh medium lacking antifolates for recovery. We also added nocodozole to the recovery medium to block cells in G_2, thereby limiting our analysis of DNA recovery to a single round of replication. Cells were collected at timed intervals throughout the experiment and were analyzed for the presence of replication intermediates. Results of these experiments are presented in Fig. 5. Upon drug treatment, a time-dependent increase in replication intermediates was observed in the p*GAL-empty*, p*GAL-DUT1*, and p*GAL-UNG1* strains (Fig. 5*A*). When released from drug, the p*GAL-DUT1* strain is able to complete synthesis of DNA with normal structure, as indicated by the reappearance of intact, migrating DNA. However, the p*GAL-empty* and p*GAL-UNG1* strains fail to complete synthesis of DNA with normal structure after drug withdraw. These data suggest that aberrant uracil-DNA repair induced by antifolates leads to defective chromosomal structures (resulting from single- and double-strand breaks) that are nonrecoverable and result in lethality. Inhibition of uracil-DNA repair (p*GAL-Ugi*) allows cells to traverse through replication with uracil-substituted DNA of normal structure. Results obtained from the Δ*ung1* strain are identical to p*GAL-Ugi* and are not shown. Fig. 5*B* shows the quantitation of chromosomal DNA from Fig. 5*A*.

DISCUSSION

dUTP Pool Accumulation Is Required for Extreme Toxicity during Thymineless Conditions. Evidence supporting dUTP accumulation and uracil misincorporation as a mechanism of thymineless toxicity has been reported in a number of model systems; however, it is still unclear to what extent this pathway contributes to lethality (3). Elevated dUTP levels have been detected in human cell lines treated with inhibitors of thymidylate metabolism; however, some cell lines tested were not able to accumulate dUTP, yet were still sensitive to TS inhibition. It has been proposed that imbalance of other nucleotides (*i.e.*, elevated levels of dATP) may contribute to cell killing by these drugs (8).

Our experiments in *S. cerevisiae* demonstrate that although all strains examined experience dTTP pool depletion during antifolate

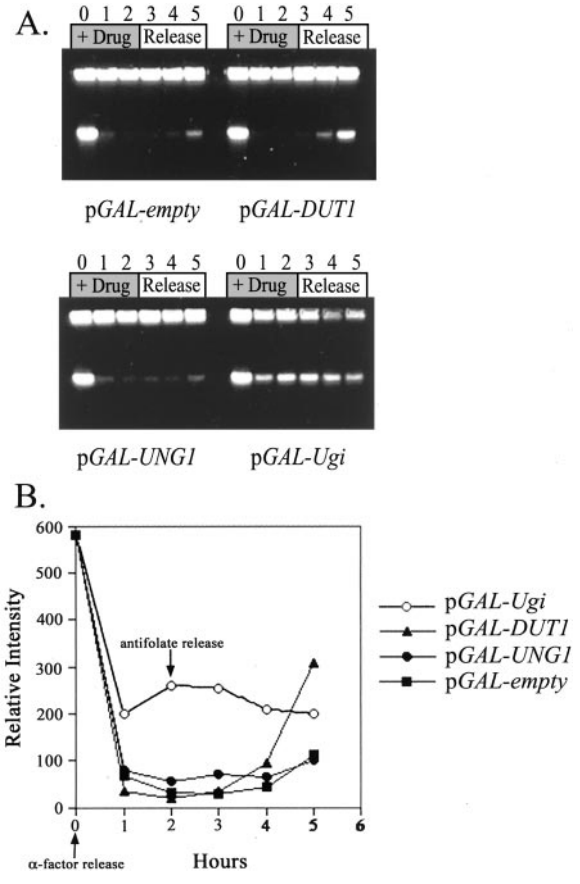

Fig. 5. Differences in the ability to recover from DNA replicational stress after transient antifolate treatment. Cells were treated with 1.5 mM α-factor for 4 h to synchronize cells in G_1 phase. Cells were then washed and transferred to fresh medium containing A + S and incubated for 2 h. Cells were then released from antifolates and transferred to fresh medium containing 10 μg/ml nocodazole. At timed intervals, cells were harvested and washed, and a determined number of cells were analyzed by PFGE. *A*, CHEF gel of chromosomes from strains transiently treated with antifolates; BMY106 (Δ*dut1::HIS3* + pBAM11 + pPS293), BMY107 (Δ*dut1::HIS3* + pBAM11 + p*GAL-DUT1*), BMY108 (Δ*dut1::HIS3* + pBAM11 + p*GAL-UNG1*), and BMY109 (Δ*dut1::HIS3* + pBAM11 + p*GAL-Ugi*). The headings over the lanes indicate at which time points that antifolates were present (*shaded headings*, + *Drug*) or when the drug had been washed out (*open headings*, *Release*). *B*, quantitation of replicated chromosomes from: ■, BMY106 (Δ*dut1::HIS3* + pBAM11 + pPS293); ▲, BMY107 (Δ*dut1::HIS3* + pBAM11 + p*GAL-DUT1*); ●, BMY108 (Δ*dut1::HIS3* + pBAM11 + p*GAL-UNG1*); and ○, BMY109 (Δ*dut1::HIS3* + pBAM11 + p*GAL-Ugi*). Quantitation of the chromosomal DNA was determined by Eagle Eye software (Stratagene).

treatment, only those that accumulate dUTP undergo severe cytotoxicity. In addition, the ability to accumulate dUTP pools is directly related to dUTPase activity levels within the cell. Cells with diminished dUTPase activity are highly sensitive to antifolate treatment, whereas overexpression of dUTPase greatly reduces sensitivity to treatment. Despite the involvement of uracil misincorporation in thymineless death, this mechanism does not account for all lethality observed in antifolate-treated cells. Even when dUTP pools do not accumulate, a significant loss of viability is observed (30% cell kill observed after 6 h of continuous exposure in the p*GAL-DUT1* strain; see Fig. 1). The mechanism of this limited, dUTP-independent toxicity is unclear; however, it may be related to the consequences of global nucleotide imbalance or prolonged checkpoint arrest.

Cellular Responses to Uracil Misincorporation. Previous investigations have noted perturbations in the cell cycle in response to inhibition of thymidylate biosynthesis (27). Our experiments show that antifolate treatment can elicit three distinct cellular responses that are directly related to dUTP status and a functional uracil-DNA repair system. When dTTP pools are depleted and dUTP pools accumulate, leading to uracil misincorporation into DNA, yeast cells are most sensitive to antifolate treatment. The immediate consequences of uracil misincorporation and detrimental repair are early S-phase arrest and formation of persistent replication intermediates. The early S-phase arrest and lethality in this case are associated with DNA damage induced by uracil-DNA repair. *ung1* deletion mutants bypass this checkpoint and complete replication with stably misincorporated uracil, providing both genetic and biochemical evidence supporting a repair-dependent mechanism. Our experiments suggest that, despite checkpoint arrest to allow for repair of damaged DNA, lethality coincides with the inability to recover from *UNG1*-initiated catastrophic damage.

Cells that do not accumulate dUTP pools during antifolate exposure demonstrate remarkable resistance to cytotoxicity. This suggests that accumulation of dUTP is the central determinant of lethality, and although required, dTTP depletion is not sufficient to mediate extreme toxicity. The accumulation of dUTP pools is dependent on several factors; however, the central regulator is likely to be dUTPase. Indeed, lowering dUTPase activity 5-fold below endogenous levels in BMY66 greatly sensitized this strain to antifolate-induced cytotoxicity. It is also likely that enzymes contributing to dUMP pool expansion or efflux during the dTTP-depleted state also determine the ultimate capacity of cells to expand dUTP pools. Despite the mechanisms involved, if dUTPase levels are sufficient to combat dUTP pool expansion during antifolate exposure, the cell is starved for a thymidine equivalent (dTTP and dUTP) for replication and responds by arresting in early S-phase. Our experiments suggest that cell cycle arrest under these conditions is likely attributable to nucleotide depletion or imbalance. *ung1* deletion mutants also arrest in early S-phase when dUTP pools are suppressed by dUTPase overexpression, suggesting a uracil repair-independent mechanism of checkpoint activation (Fig. 3*F*). In sharp contrast to cells that experience detrimental uracil misincorporation/repair, those that do not accumulate dUTP are able to recover from the early S-phase arrest when drug is withdrawn. These cells demonstrate the ability to complete DNA synthesis, producing chromosomes of normal structure. This suggests that enhanced survival observed in cells that do not accumulate dUTP is related to the ability to effectively recover from replicational stress.

The effect of inactivating uracil-DNA repair during antifolate treatment was dramatic, not only in terms of lethality, but also in a distinct checkpoint response. Deletion or inhibition of the *UNG1* gene product led to short-term enhancement of viability after antifolate exposure. These cells were able to complete DNA replication using uracil in place of thymidine. Upon the completion of replication, these cells arrested in G_2-M and exhibited toxicity at later time points. The mechanism that leads to checkpoint arrest is unclear. It is possible that stably incorporated uracil residues in DNA may be signaling the checkpoint. Uracil-containing DNA has an inherently different stacking structure than normal DNA (28), and it has been also reported that transcription factors are unable to bind to their target sequences if uracil is present (29). Alternatively, it is possible that other promiscuous repair activities acting on uracil residues could be initiating low-level DNA damage that induces the G_2-M arrest. Further clarification of this issue awaits future studies using both DNA repair and cell cycle checkpoint mutants.

The Role of Uracil-DNA Metabolism in Therapeutics. Thymidylate metabolism is an important target for widely used chemotherapeutic agents used to treat many types of cancer in addition to some forms of arthritis and bacterial and fungal infections. Although this pathway has been targeted for many years, the mechanisms of drug action resulting in toxicity are still unclear. Studies implicating uracil misincorporation in cancer cell lines subsequent to TS inhibition suggest that this mechanism may have an important role in early

toxicity (within 24 h; Ref. 8). When dUTP accumulation is suppressed in HT29 human colon cancer cells by overexpression of dUTPase activity, toxicity is delayed (13). This observation may have important implications in the clinical setting, where it is often more difficult to maintain high concentrations of antimetabolite within the tumor over extended periods of time. If this is the case, early toxicity elicited by uracil misincorporation may be the ultimate determinant of clinical efficacy. We demonstrate that lowering dUTPase activity in budding yeast greatly sensitizes cells to the effects of TS inhibition, providing a basis for further validation studies for dUTPase as a target for drug development. Furthermore, our studies strongly suggest that efficacy to TS-directed therapeutics can be greatly influenced by the expression of dUTPase and uracil-DNA glycosylase. Indeed, dUTPase expression in the nucleus of colon cancer cells has been implicated as a prognostic marker for resistance to 5-fluorouracil in metastatic colon cancer (30).

In conclusion, we provide definitive biochemical evidence implicating aberrant uracil-DNA metabolism as the central mediator of thymineless death in yeast. Our data further establish a link between the levels of dUTPase and uracil-DNA glycosylase and lethality elicited by antifolates. Although these data clearly define an association between toxicity and mechanism, the significance of uracil misincorporation in mediating response to chemotherapy in human cancers remains to be resolved.

ACKNOWLEDGMENTS

We thank Michael Henry for the generous gifts of yeast strains and plasmids as well as technical assistance. We thank Sara Koehler and Michael Mandola for critical reading of the manuscript, William Fazzone for assistance in generating figures, and Ariel Meyer for technical assistance.

REFERENCES

1. Moertel, C. G. Chemotherapy for colorectal cancer [see comments]. N. Eng. J. Med., *330:* 1136–1142, 1994.
2. Goulian, M., Bleile, B., and Tseng, B. Y. The effect of methotrexate on levels of dUTP in animal cells. J. Biol. Chem., *255:* 10630–10637, 1980.
3. Kunz, B. A., Kohalmi, S. E., Kunkel, T. A., Mathews, C. K., McIntosh, E. M., and Reidy, J. A. Deoxyribonucleoside triphosphate levels: a critical factor in the maintenance of genetic stability. Mutat. Res., *318:* 1–64, 1994.
4. Houghton, J. A., Harwood, F. G., and Houghton, P. J. Cell cycle control processes determine cytostasis or cytotoxicity in thymineless death of colon cancer cells. Cancer Res., *54:* 4967–4973, 1994.
5. Houghton, J. A., Tillman, D. M., and Harwood, F. G. Ratio of 2′-deoxyadenosine-5′-triphosphate/thymidine-5′-triphosphate influences the commitment of human colon carcinoma cells to thymineless death. Clin. Cancer Res., *1:* 723–730, 1995.
6. Chong, L. K., and Tattersall, M. H. 5,10-Dideazatetrahydrofolic acid reduces toxicity and deoxyadenosine triphosphate pool, expansion in cultured L1210 cells treated with inhibitors of thymidylate synthase. Biochem. Pharmacol., *49:* 819–827, 1995.
7. Wataya, Y., Hwang, H., Nakazawa, T., Takahashi, K., Otani, M., and Igaki, T. Molecular mechanism of cell death induced dNTP pool imbalance. Nucleic Acids Symp. Ser., 109–110, 1993.
8. Aherne, G. W., and Browne, S. The role of uracil misincorporation in thymineless death. *In:* A. L. Jackman (ed.), Anticancer Drug Development Guide: Antifolate Drugs in Cancer Therapy, pp. 409–421. Totowa, NJ: Humana Press, Inc., 1999.
9. Brynolf, K., Eliasson, R., and Reichard, P. Formation of Okazaki fragments in polyoma DNA synthesis caused by misincorporation of uracil. Cell, *13:* 573–580, 1978.
10. Gadsden, M. H., McIntosh, E. M., Game, J. C., Wilson, P. J., and Haynes, R. H. dUTP pyrophosphatase is an essential enzyme in *Saccharomyces cerevisiae*. EMBO J., *12:* 4425–4431, 1993.
11. Kunz, B. A. Inhibitors of thymine nucleotide biosynthesis: antimetabolites that provoke genetic change via primary non-DNA targets. Mutat. Res., *355:* 129–140, 1996.
12. Sedwick, W. D., Kutler, M., and Brown, O. E. Antifolate-induced misincorporation of deoxyuridine monophosphate into DNA: inhibition of high molecular weight DNA synthesis in human lymphoblastoid cells. Proc. Natl. Acad. Sci. USA, *78:* 917–921, 1981.
13. Canman, C. E., Radany, E. H., Parsels, L. A., Davis, M. A., Lawrence, T. S., and Maybaum, J. Induction of resistance to fluorodeoxyuridine cytotoxicity and DNA damage in human tumor cells by expression of *Escherichia coli* deoxyuridinetriphosphatase. Cancer Res., *54:* 2296–2298, 1994.
14. Webley, S. D., Hardcastle, A., Ladner, R. D., Jackman, A. L., and Aherne, G. W. Deoxyuridine triphosphatase (dUTPase) expression and sensitivity to the thymidylate synthase (TS) inhibitor ZD9331. Br. J. Cancer, *83:* 792–799, 2000.
15. Barclay, B. J., Kunz, B. A., Little, J. G., and Haynes, R. H. Genetic and biochemical consequences of thymidylate stress. Can. J. Biochem., *60:* 172–184, 1982.
16. Burke, D., Dawson, D., and Stearns, T. Methods in Yeast Genetics. Plainview, NY: Cold Spring Harbor Laboratory, 2000.
17. Sherman, P. A., and Fyfe, J. A. Enzymatic assay for deoxyribonucleoside triphosphates using synthetic oligonucleotides as template primers. Anal. Biochem., *180:* 222–226, 1989.
18. Horowitz, R. W., Zhang, H., Schwartz, E. L., Ladner, R. D., and Wadler, S. Measurement of deoxyuridine triphosphate and thymidine triphosphate in the extracts of thymidylate synthase-inhibited cells using a modified DNA polymerase assay. Biochem. Pharmacol., *54:* 635–638, 1997.
19. Caradonna, S., Ladner, R., Hansbury, M., Kosciuk, M., Lynch, F., and Muller, S. Affinity purification and comparative analysis of two distinct human uracil-DNA glycosylases. Exp. Cell Res., *222:* 345–359, 1996.
20. Sazer, S., and Sherwood, S. W. Mitochondrial growth and DNA synthesis occur in the absence of nuclear DNA replication in fission yeast. J. Cell Sci., *97* (Pt. 3)*:* 509–516, 1990.
21. Baudin, A., Ozier-Kalogeropoulos, O., Denouel, A., Lacroute, F., and Cullin, C. A simple and efficient method for direct gene deletion in *Saccharomyces cerevisiae*. Nucleic Acids Res., *21:* 3329–3330, 1993.
22. Ladner, R. D., McNulty, D. E., Carr, S. A., Roberts, G. D., and Caradonna, S. J. Characterization of distinct nuclear and mitochondrial forms of human deoxyuridine triphosphate nucleotidohydrolase. J. Biol. Chem., *271:* 7745–7751, 1996.
23. Haushalter, K. A., Todd Stukenberg, M. W., Kirschner, M. W., and Verdine, G. L. Identification of a new uracil-DNA glycosylase family by expression cloning using synthetic inhibitors. Curr. Biol., *9:* 174–185, 1999.
24. Reddy, S. M., Williams, M., and Cohen, J. I. Expression of a uracil DNA glycosylase (UNG) inhibitor in mammalian cells: varicella-zoster virus can replicate *in vitro* in the absence of detectable UNG activity. Virology, *251:* 393–401, 1998.
25. Barclay, B. J., and Little, J. G. Genetic damage during thymidylate starvation in *Saccharomyces cerevisiae*. Mol. Gen. Genet., *160:* 33–40, 1978.
26. Desany, B. A., Alcasabas, A. A., Bachant, J. B., and Elledge, S. J. Recovery from DNA replicational stress is the essential function of the S-phase checkpoint pathway. Genes Dev., *12:* 2956–2970, 1998.
27. Webley, S. D., Welsh, S. J., Jackman, A. L., and Aherne, G. W. The ability to accumulate deoxyuridine triphosphate and cellular response to thymidylate synthase (TS) inhibition. Br. J. Cancer, *85:* 446–452, 2001.
28. Miller, K. J., and Savchik, J. A. A new empirical method to calculate average molecular polarizabilities. J. Am. Chem. Soc., *101:* 7206–7213, 1979.
29. Pu, W. T., and Struhl, K. Uracil interference, a rapid and general method for defining protein-DNA interactions involving the 5-methyl group of thymines: the GCN4-DNA complex. Nucleic Acids Res., *20:* 771–775, 1992.
30. Ladner, R. D., Lynch, F. J., Groshen, S., Xiong, Y. P., Sherrod, A., Caradonna, S. J., Stoehlmacher, J., and Lenz, H. J. dUTP nucleotidohydrolase isoform expression in normal and neoplastic tissues: association with survival and response to 5-fluorouracil in colorectal cancer. Cancer Res., *60:* 3493–3503, 2000.